

# Gain enhancement of an electrically small antenna array using metamaterials

Bratin Ghosh · Susmita Ghosh

Received: 1 March 2010 / Accepted: 19 July 2010 / Published online: 18 August 2010  
© Springer-Verlag 2010

**Abstract** This paper presents the enhancement of radiated power ratio of a two-dipole array of infinitesimal dipole elements, separated by an infinitesimal distance. It is shown that a properly constructed metamaterial shell configuration with optimized material parameters surrounding the dipole can cancel both the self- and the mutual reactances of the array system. Simultaneously, a very high radiated power ratio is realized for the array system even in the presence of strong mutual coupling between the array elements. This potentially leads to the development of highly efficient ultra-compact antenna arrays. In addition, by using a material of non-unity permittivity surrounding the array system, uniform radiated power ratio characteristics can be achieved with the variation in the metamaterial shell thickness. This removes the major drawback in the practical design of the metamaterial shell proposed earlier for the radiated power ratio enhancement of a single dipole. Very good matching characteristics are obtained for the antenna configuration demonstrating almost complete cancelation of the reactive power of the array system. The frequency dispersive behavior of the antenna configuration is investigated using the lossless and lossy Drude models.

## 1 Introduction

Electrically small antennas and antenna efficiency have been an area of active research in the past and present [1–5]. A detailed list of other references in this topic appears in [1, 2]. It was shown in [1] that a high radiated power ratio was possible for the electrically small dipole by compensating the large capacitive reactance by the inductive reactance of a double-negative (DNG) shell surrounding the dipole. The inductive impedance offered by the DNG shell was caused due to a change in sign of the reactive part of the complex power radiated by the infinitesimal dipole in an infinite DNG medium. Practically, the DNG shell can be realized using a wire and split-ring resonator (SRR) topology [6], capacitively loaded strips with SRR [7] or other metamaterial configurations addressed in the literature. In the following work it is shown that a DNG shell can also be used to achieve a high radiated power ratio for a two-element array of infinitesimal dipoles. The result is particularly significant as in addition to the self-reactance of the individual dipoles, a strong mutual reactance is present between the infinitesimal dipole elements which are spaced an infinitesimal distance apart. Thus, unlike the case of the single dipole surrounded by a metamaterial shell in [1] where only the self-reactance of the dipole has to be canceled by the reactance of the metamaterial shell, both the self- and mutual reactances has to be tuned out by the DNG shell for the case of the two-element dipole array.

It is first shown that the reactive part of the complex power changes sign when the two-dipole array is placed in an unbounded DNG medium relative to that in an unbounded double-positive (DPS) medium. This demonstrates the feasibility of designing a self-resonant antenna configuration for the enhancement of the radiated power ratio for the two-dipole system using a DNG shell. It is next demonstrated that a suitable DNG shell can indeed be designed

---

B. Ghosh (✉) · S. Ghosh  
Department of Electronics and Electrical Communication  
Engineering, Indian Institute of Technology, Kharagpur,  
West Bengal 721 302, India  
e-mail: [bghosh@ece.iitkgp.ernet.in](mailto:bghosh@ece.iitkgp.ernet.in)  
Fax: +91-3222255303

S. Ghosh  
e-mail: [susmita.gh@gmail.com](mailto:susmita.gh@gmail.com)

to enhance the radiated power ratio of the array by a very large order of magnitude by cancelation of both the self- and the mutual reactances of the dipole array, potentially leading to the development of ultra-compact arrays. The other significant feature of the current work is the achievement of uniformity in the radiated power ratio characteristics over a large range of shell thickness. This alleviates one of the major limitations towards the practical design of the metamaterial shell reported in [1] and addressed in [5] for a single antenna element. The resonance behavior of the configuration with change in frequency is also investigated using the lossy and the lossless Drude models.

### 2 Analysis of two-element dipole array surrounded by a DNG shell

The antenna topology is shown in Fig. 1. The two dipoles linearly displaced along the  $z$ -axis by equal and opposite displacements from the center are surrounded by a DNG shell (Region 2) of permittivity  $\epsilon_{r2}$  and permeability  $\mu_{r2}$ . The length of the dipoles and their relative separation are denoted by ‘ $l$ ’ and ‘ $s$ ’ respectively, with the dipole current  $I_0$ . The permittivity and permeability of Region 1 are  $\epsilon_{r1}$  and  $\mu_{r1}$  respectively, with Region 3 being free space.

Similar to the investigation of enhancement of radiated power ratio of a single infinitesimal dipole in [1], it is first demonstrated that the reactive component of the complex power changes sign when the infinitesimal two-dipole array is placed in an infinite DNG medium, where the wavenumber  $k$  is negative, relative to the complex power radiated in a unbounded DPS medium, where  $k$  is positive. The shell is not present in this case. Assuming the dipole separation

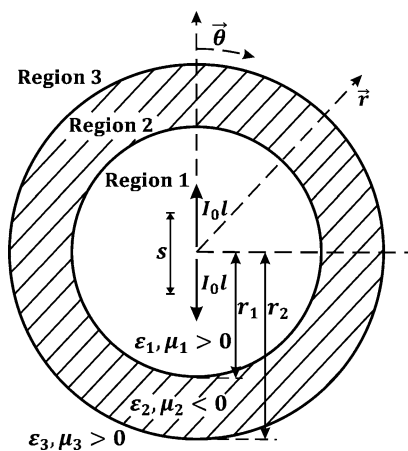


**Fig. 1** Two-element infinitesimal dipole array surrounded by a DNG shell

‘ $s$ ’ to be very small, the magnetic vector potential can be written from pp. 288 of [8] as

$$A_z = \frac{k^2 I_0 l s}{4\pi j} h_1^{(2)}(kr) P_1(\cos \theta) \tag{1}$$

where  $h_1^{(2)}$  represents the first-order spherical Hankel function of the second kind and  $P_1(\cos \theta)$  is the Legendre polynomial of the first kind and first order. The electric and magnetic field components of the dipole system,  $E_\theta$  and  $H_\phi$  in an unbounded DPS medium, can be computed from (1) and are given by

$$E_\theta = -\frac{k^4 I_0 l s}{4\pi \omega \epsilon} \sin \theta \cos \theta h_1^{(2)''}(kr) \tag{2}$$

$$H_\phi = \frac{k^2 I_0 l s}{4\pi j r} \sin \theta \cos \theta [h_1^{(2)}(kr) - kr h_1^{(2)'}(kr)] \tag{3}$$

where the derivatives are with respect to the function arguments. Also, in the above,  $h_1^{(2)'}(kr)$  and  $h_1^{(2)''}(kr)$  are the first and second derivatives respectively of the spherical Hankel functions. From (2) and (3), the complex radiated power by the dipole array is evaluated as

$$P = \frac{1}{2} \int_0^{2\pi} \int_0^\pi E_\theta H_\phi^* r^2 \sin \theta d\theta d\phi = \frac{-jk^5 I_0^2 l^2 s^2 r \sqrt{\mu} h_1^{(2)''}(kr) \{h_1^{(2)*}(kr) - kr h_1^{(2)'}(kr)\}}{60\pi \sqrt{\epsilon}} \tag{4}$$

where  $h_1^{(2)*}(kr)$  is the complex conjugate of the spherical Hankel function. After simplifying and evaluating the derivative terms in (4), we obtain

$$P = \frac{-jk^4 I_0^2 l^2 s^2 r \sqrt{\mu}}{60\pi \sqrt{\epsilon}} \times \left[ 2k |h_0^{(2)}(kr)|^2 - \left\{ 3 |h_1^{(2)}(kr)|^2 \left( k - \frac{6}{kr^2} \right) \right\} + kr \left( k - \frac{6}{kr^2} \right) h_0^{(2)*}(kr) h_1^{(2)}(kr) - \frac{6}{r} h_0^{(2)}(kr) h_1^{(2)*}(kr) \right] = \frac{I_0^2 l^2 s^2 \sqrt{\mu}}{60\pi \sqrt{\epsilon}} \left[ k^4 - \frac{3j}{r^3} \left\{ k + \frac{6}{kr^2} \right\} \right] \tag{5}$$

$h_0^{(2)}$  and  $h_0^{(2)*}(kr)$  being the zeroth order spherical Hankel function of the second kind and its complex conjugate respectively. It is seen from (5) that the reactive part of the complex power  $P$  is an odd function of  $k$  while the real part of  $P$  is an even function of  $k$ . Thus, it can be seen that the reactive part of  $P$  changes sign when the two-dipole system is

placed in a DNG medium, while the real part of  $P$  retains its sign by causality. This implies that it should be possible to design a self-resonant antenna system by compensating both the self- and mutual reactances of the two-dipole system.

Considering now the structure in Fig. 1, the total electric and magnetic fields in Region 1 can be considered as a superposition of the incident field from the dipoles and the scattered field from the shell. The tangential electric and magnetic fields in the three regions are obtained from (1) and given as follows:

Region 1:

$$H_{\phi}^1 = \frac{k_1^2 I_0 l s}{4\pi j r} \sin\theta \cos\theta [h_1^{(2)}(k_1 r) - k_1 r h_1^{(2)'}(k_1 r)] + \frac{C_1}{r} \sin\theta \cos\theta [j_1(k_1 r) - k_1 r j_1'(k_1 r)] \quad (6)$$

$$E_{\theta}^1 = -\frac{k_1^4 I_0 l s}{4\pi \omega \varepsilon_1} \sin\theta \cos\theta h_1^{(2)''}(k_1 r) + \frac{C_1 k_1^2}{j \omega \varepsilon_1} j_1''(k_1 r) \sin\theta \cos\theta \quad (7)$$

Region 2:

$$H_{\phi}^2 = \frac{C_2}{r} \sin\theta \cos\theta [(j_1(k_2 r) + C_3 n_1(k_2 r)) - k_2 r (j_1'(k_2 r) + C_3 n_1'(k_2 r))] \quad (8)$$

$$E_{\theta}^2 = \frac{C_2 k_2^2}{j \omega \varepsilon_2} \sin\theta \cos\theta [j_1''(k_2 r) + C_3 n_1''(k_2 r)] \quad (9)$$

Region 3:

$$H_{\phi}^3 = \frac{C_4}{r} \sin\theta \cos\theta [h_1^{(2)}(k_3 r) - k_3 r h_1^{(2)'}(k_3 r)] \quad (10)$$

$$E_{\theta}^3 = \frac{C_4 k_3^2}{j \omega \varepsilon_3} \sin\theta \cos\theta h_1^{(2)''}(k_3 r) \quad (11)$$

In the above, the terms  $j_1(k_1 r)$ ,  $j_1'(k_1 r)$  and  $j_1''(k_1 r)$  represent the first-order spherical Bessel function of the first kind, its first derivative and its second derivative respectively. Also, the terms  $n_1(k_2 r)$ ,  $n_1'(k_2 r)$  and  $n_1''(k_2 r)$  refer to the first-order spherical Bessel function of the second kind, its first and second derivatives respectively. The unknown coefficients  $C_1$ – $C_4$  are obtained by enforcing the continuity of the tangential field components across the dielectric interfaces at  $r = r_1$  and  $r = r_2$  and are given as follows:

$$C_1 = \frac{-[X_1 X_3 + X_2]}{[(j_1(k_1 r_1) - k_1 r_1 j_1'(k_1 r_1)) - X_3 k_1^2 j_1''(k_1 r_1)]} \quad (12)$$

$$C_2 = \frac{C_1 k_1^2 j_1''(k_1 r_1) - X_1}{\frac{\varepsilon_1 k_2^2}{\varepsilon_2} [j_1''(k_2 r_1) + C_3 n_1''(k_2 r_1)]} \quad (13)$$

$$C_3 = \frac{X_4 (\frac{\varepsilon_3 k_2^2}{\varepsilon_2} j_1''(k_2 r_2)) - (k_3^2 h_1^{(2)''}(k_3 r_2)) (j_1(k_2 r_2) - k_2 r_2 j_1'(k_2 r_2))}{(k_3^2 h_1^{(2)''}(k_3 r_2)) (n_1(k_2 r_2) - r_2 k_2 n_1'(k_2 r_2)) - X_4 (\frac{\varepsilon_3 k_2^2}{\varepsilon_2} n_1''(k_2 r_2))} \quad (14)$$

$$C_4 = \frac{\varepsilon_3 k_2^2}{\varepsilon_2 k_3^2} C_2 \frac{[j_1''(k_2 r_2) + C_3 n_1''(k_2 r_2)]}{h_1^{(2)''}(k_3 r_2)} \quad (15)$$

where

$$X_1 = j \frac{k_1^4 I_0 l s}{4\pi} h_1^{(2)''}(k_1 r_1) \quad (16)$$

$$X_2 = \frac{k_1^2 I_0 l s}{4\pi j} [h_1^{(2)}(k_1 r_1) - k_1 r_1 h_1^{(2)'}(k_1 r_1)] \quad (17)$$

$$X_3 = \frac{(j_1(k_2 r_1) + C_3 n_1(k_2 r_1)) - k_2 r_1 (j_1'(k_2 r_1) + C_3 n_1'(k_2 r_1))}{\frac{\varepsilon_1 k_2^2}{\varepsilon_2} [j_1''(k_2 r_1) + C_3 n_1''(k_2 r_1)]} \quad (18)$$

$$X_4 = h_1^{(2)}(k_3 r_2) - k_3 r_2 h_1^{(2)'}(k_3 r_2) \quad (19)$$

In the above,  $k_1$ ,  $k_2$  and  $k_3$  refer to the wavenumbers in Regions 1, 2 and 3 respectively and are given by  $k_n = \omega \sqrt{\mu_n \varepsilon_n}$ ,  $n = 1, 2, 3$ .

The radiated power ratio [2] of the two-dipole system can be computed from the above field expressions and is given by

*Radiated power ratio*

$$= \frac{-16\pi^2 r |C_4|^2 \text{Re}\{j h_1^{(2)''}(k_0 r) \{h_1^{(2)*}(k_0 r) - k_0 r h_1^{(2)*/'}(k_0 r)\}\}}{k_0^3 I_0^2 l^2 s^2} \quad (20)$$

where  $k_0 = \omega \sqrt{\mu_0 \varepsilon_0}$  refer to the wavenumber of free space. In (20), the radiated power ratio is given by the ratio of the power radiated by the antenna system in the presence of the DNG shell to the power radiated by the same antenna system in free space ( $P_{\text{radfree space}}$ ), the latter quantity being given by  $P_{\text{radfree space}} = \frac{k_0^4 \eta_0 I_0^2 l^2 s^2}{60\pi}$ , where  $\eta_0$  is the intrinsic impedance of free space.

### 3 Results

The antenna configuration was designed for operation at 10 GHz. The dipole lengths were chosen to be  $l = \frac{\lambda_0}{1000} = 0.03$  mm with the dipole separation  $s = 0.04$  mm and the dipole current  $I_0 = 1$  A. The media parameters in Sect. 2 were optimized to obtain a high radiated power ratio for the antenna structure. It should be noted at first that a high and uniform radiated power ratio could only be obtained for the case of a single dipole surrounded by a DNG shell in [5] by choosing a non-unity permittivity for the inner medium. It

should also be noted that though a uniform radiated power ratio is obtained over a much larger shell thickness, the frequency bandwidth of the system is narrow as is seen when dispersion is taken into account through the Drude model. The enhancement of radiated power ratio of the two-dipole system was investigated with variation in the permittivity  $\epsilon_{r2}$  of the DNG shell with  $\epsilon_{r1}$  as a parameter and shown in Fig. 2(a). The permeabilities  $\mu_{r1}$  and  $\mu_{r2}$  were maintained at 1 and  $-1$  respectively, consistent with [5]. It is seen that corresponding to any value of permittivity  $\epsilon_{r1}$  in Region 1, the permittivity  $\epsilon_{r2}$  of the DNG shell can be appropriately selected to achieve a large radiated power ratio. The case  $\epsilon_{r1} = 1$  has not been shown as more than one scattered mode has to be used in the formulation in this case. This case is also not considered to be optimum as the required DNG shell thickness for achieving a high radiated power ratio is extremely small as noted in Fig. 11 of [1]. Further, as excellent radiated power ratio characteristics are obtained with other values of  $\epsilon_{r1}$ , this case is not treated further. The inner and outer radii of the DNG shell have been maintained at  $r_1 = 0.10$  mm and  $r_2 = 0.75$  mm respectively. It can be seen from Fig. 2(a) that the best radiated power ratio characteristics are obtained for the permittivities  $\epsilon_{r1} = 3$  and  $\epsilon_{r2} = -2$ . Figure 2(b) shows the effect of a parametric variation of permeabilities of Region 1 and 2 on the radiated

power ratio characteristics, with the optimized parameters  $\epsilon_{r1} = 3$  and  $\epsilon_{r2} = -2$  from above. It can be seen that higher values of the peak in the radiated power ratio are obtained as the permeability of Region 1 decreases.

It might be noted that the two-dipole structure under consideration exhibits quadrupole resonance, similar to a single dipole structure surrounded by a metamaterial shell reported in [9]. It has been shown in [9], (15) that a quadrupole resonance can be obtained for such a structure by substituting  $n = 2$  for the eigenvalue  $n$ . It can be verified that the resonant peaks in Figs. 2(a) and (b) are located very close to the quadrupole resonances predicted by (15a) and (15b) in [9] for the chosen material parameters and ratio of radii of the outer and inner shells. For example, for the chosen dimensions of the shell in Fig. 2(a), the values of  $\epsilon_{r2}$  predicted by (15a) of [9] for the quadrupole resonances are  $-1.5022, -2.0013, -2.6675, -3.3342$  and  $-4.0008$  corresponding to  $\epsilon_{r1} = 2, 3, 4, 5$  and  $6$  respectively. In comparison, the radiated power ratio peaks in Fig. 2(a) are seen to occur at  $\epsilon_{r2} = -1.4, -2.0, -2.6, -3.3$  and  $-4.0$ , which can be observed to be close to the quadrupole resonances. Similar behavior can be verified for Fig. 2(b), using (15b) of [9] to compute the resonant values of  $\mu_{r2}$ .

Next, in order to determine the optimum dimensions of the DNG shell, the variation of radiated power ratio is investigated in Fig. 3(a) with change in the outer radius  $r_2$  of the

**Fig. 2** Variation in the radiated power ratio of the two-element dipole array with DNG shell permittivity and permeabilities.  $r_1 = 0.10$  mm,  $r_2 = 0.75$  mm. (a) Radiated power ratio vs.  $\epsilon_{r2}$  for different values of  $\epsilon_{r1}$ ,  $\mu_{r1} = 1, \mu_{r2} = -1$ . (b) Radiated power ratio vs.  $\mu_{r2}$  for different values of  $\mu_{r1}$ ,  $\epsilon_{r1} = 3$  and  $\epsilon_{r2} = -2$

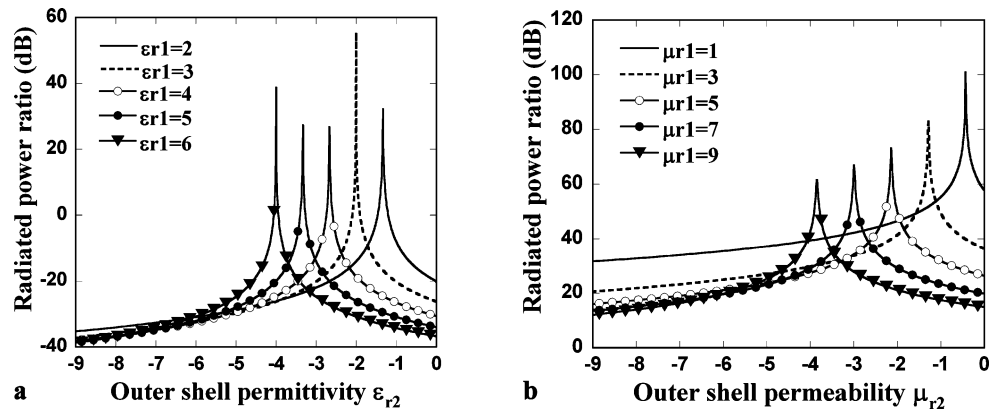


**Fig. 3** (a) Radiated power ratio and (b) reactance ratio of a two-element dipole array surrounded by a DNG shell with different values of permeabilities in Region 2 and variable outer radius  $r_2$  with inner radius  $r_1 = 0.10$  mm,  $\epsilon_{r1} = 3, \mu_{r1} = 1$  and  $\epsilon_{r2} = -2$

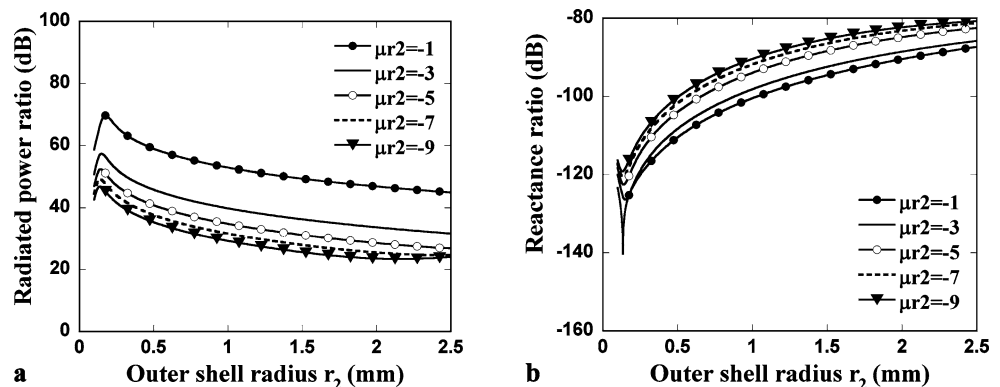


**Fig. 4** (a) Radiated power ratio and (b) reactance ratio of a two-element dipole array surrounded by a DNG shell with different values of permeabilities in Region 1 and variable outer radius  $r_2$  with inner radius  $r_1 = 0.10$  mm,  $\varepsilon_{r1} = 3$ ,  $\varepsilon_{r2} = -2$  and  $\mu_{r2} = -1$

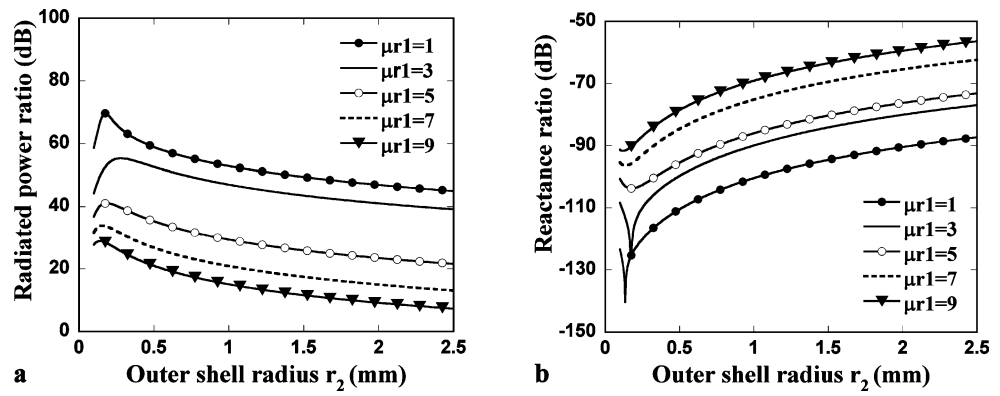
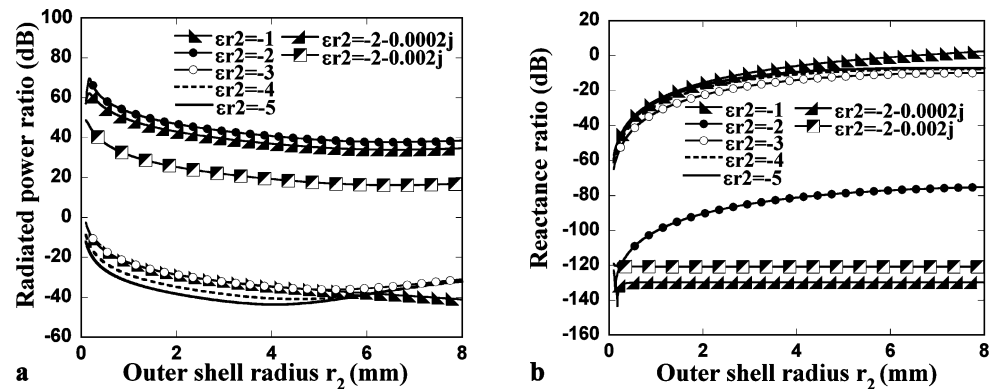


**Fig. 5** (a) Radiated power ratio and (b) reactance ratio of a two-element dipole array surrounded by a DNG shell with different values of permittivities in Region 2 and variable outer radius  $r_2$  with inner radius  $r_1 = 0.10$  mm,  $\varepsilon_{r1} = 3$ ,  $\mu_{r1} = 1$  and  $\mu_{r2} = -1$



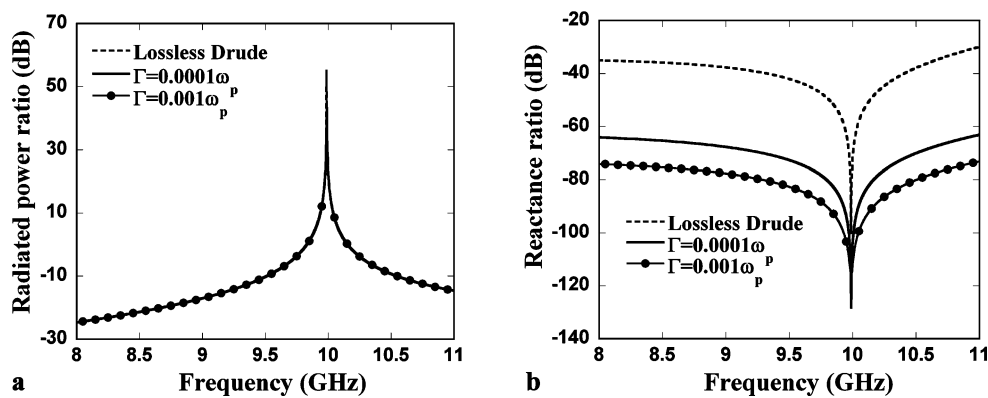
shell, keeping the inner radius  $r_1$  fixed at 0.10 mm. The media parameters  $\varepsilon_{r1} = 3$ ,  $\mu_{r1} = 1$  and  $\varepsilon_{r2} = -2$  were chosen based on the previous optimization, with  $\mu_{r2}$  as a variable parameter. It can be observed that uniform radiated power ratio characteristics are obtained as  $r_2$  varies, over a wide range of thickness of the DNG shell. As noted previously, although a high radiated power ratio was obtained in [1] for a single infinitesimal dipole surrounded by a DNG shell, one of the biggest challenges in the practical realization of the shell was its extremely small thickness. Thicker shells could only be realized by compromising for a lower value of radiated power ratio. It was shown in [5] that it was possible to obtain a high and stable radiated power ratio characteristics for the infinitesimal dipole with much thicker shells by choosing an appropriate permittivity value different from unity for Region 1. Figure 3(a) shows that uniform radiated power ratio characteristics with simultaneously high values of radiated power ratio can be obtained for the dipole array if the material parameters in Regions 1 and 2 are chosen appropriately. The best radiated power ratio characteristics are obtained with  $\mu_{r2} = -1$  with a peak in the radiated power ratio of 69.62 dB at  $r_2 = 0.175$  mm. The corresponding reactance ratio [1] is shown in Fig. 3(b). It is observed that extremely low reactance ratio is obtained corresponding to the peak in the radiated power ratio in Fig. 3(a). This signifies almost perfect cancelation of the reactive component

of power from the dipole array thus making the infinitesimal antenna system resonant.

Next, the effect of a change in the permeability  $\mu_{r1}$  of Region 1 on the radiated power ratio versus  $r_2$  is investigated in Fig. 4 with the same inner radius  $r_1$  as in Fig. 3. The other media parameters are maintained at  $\varepsilon_{r1} = 3$ ,  $\varepsilon_{r2} = -2$  and  $\mu_{r2} = -1$ . The radiated power ratio characteristics are again gradual in nature and do not show the extreme peaked characteristics with variation in shell thickness as in Fig. 11(a) of [1]. A thicker shell can thus be fabricated, reducing the design tolerance manifold. Simultaneously, a high radiated power ratio can be realized. Optimum radiated power ratio characteristics are obtained for  $\mu_{r1} = 1$ .

The effect of variation in the permittivity  $\varepsilon_{r2}$  of the DNG shell on the radiated power ratio characteristics is investigated next. The results are shown in Fig. 5. Based on the optimized values obtained from the previous radiated power ratio characteristics, the other media parameters are chosen to be  $\varepsilon_{r1} = 3$ ,  $\mu_{r1} = 1$  and  $\mu_{r2} = -1$ . From Fig. 5, a high and stable radiated power ratio characteristic is observed for  $\varepsilon_{r2} = -2$ , with the radiated power ratio higher than 37.70 dB for  $r_2 \leq 8$  mm. In addition, it can be seen from Fig. 5(b) that the high reactive load of free space for the infinitesimal dipole array is effectively canceled at the radiated power ratio peak. The effect of finite loss-tangents 0.0001 and 0.001 in the DNG shell is also seen in Fig. 5, cor-

**Fig. 6** (a) Radiated power ratio and (b) reactance ratio versus frequency for a Drude model DNG shell for the optimized design in case of the infinitesimal two-element dipole array with  $r_1 = 0.1$  mm,  $r_2 = 0.75$  mm,  $\epsilon_{r1} = 3$ ,  $\mu_{r1} = 1$ ,  $f_{\epsilon p} = 17.3$  GHz and  $f_{\mu p} = 13$  GHz



responding to  $\epsilon_{r2} = -2 - 0.0002j$  and  $\epsilon_{r2} = -2 - 0.002j$  respectively. It can be observed from Fig. 5(a) that the radiated power ratio steadily decreases with increase in dielectric loss, as expected. However, the uniformity in the loss characteristics is preserved when the dielectric loss is considered. The parametric variation of the radiated power ratio characteristics versus  $r_2$  with change in  $\epsilon_{r1}$  is also similar to the variation in radiated power ratio with change in  $\epsilon_{r2}$  presented above and is not shown for brevity. The best radiated power ratio characteristics are obtained for the media parameters  $\epsilon_{r1} = 3$ ,  $\mu_{r1} = 1$ ,  $\epsilon_{r2} = -2$  and  $\mu_{r2} = -1$ .

The dispersive behavior of the DNG-dipole array is next investigated in Fig. 6 using the Drude model for the DNG shell. Both lossless and lossy cases are considered. The electric and magnetic plasma frequencies are set to  $f_{\epsilon p} = 17.3$  GHz and  $f_{\mu p} = 13$  GHz respectively to obtain  $\epsilon_{r2} = -2$  and  $\mu_{r2} = -1$  at the design frequency of 10 GHz. The collision frequencies were chosen to be  $\Gamma_{\epsilon} = 0.0001\omega_{p\epsilon}$ ,  $\Gamma_{\mu} = 0.0001\omega_{p\mu}$  and  $\Gamma_{\epsilon} = 0.001\omega_{p\epsilon}$ ,  $\Gamma_{\mu} = 0.001\omega_{p\mu}$  for the two cases of loss in the Drude model. The inner and outer radii of the DNG shell are fixed at  $r_1 = 0.10$  mm and  $r_2 = 0.75$  mm respectively. The lossless and lossy dispersion characteristics in Fig. 6(a) are seen to almost overlap. The peak radiated power ratios at 10 GHz for the lossless case is observed to be at 55.00 dB while those for the less and more lossy cases are at 44.27 dB and 25.44 dB respectively. The effect of an increase in the inner radius of the DNG shell on the dispersion characteristics is to decrease the Q of the antenna system as discussed in [1] and is not repeated for brevity.

It might be mentioned that the verification of the results obtained in this paper using commercially available electromagnetic simulation tools like the High-Frequency Structure Simulator (HFSS) or computation of input impedance for the antenna system could not be done due to the lack of considerably high computational resource needed for the simulation of electrically small antennas [2]. The reliability of the results is based on the fact that the results using

the same methodology for a single dipole surrounded by a metamaterial shell has been verified using HFSS in [2].

#### 4 Conclusions

The enhancement in radiated power ratio of a two-element infinitesimal dipole array is investigated using a metamaterial shell. The investigation is inspired by the enhancement in the radiated power ratio of a single infinitesimal dipole surrounded by a DNG shell, which has been reported previously. It is seen that an optimized DNG shell system can be designed to cancel both the self- and mutual reactances of the electrically small two-element dipole array. This is based on the fact that the reactive power of the two-dipole system changes sign when placed in an unbounded DNG medium compared to that in an infinite DPS medium. Simultaneously it is seen that a very high radiated power ratio is achieved for the dipole array in the presence of strong mutual coupling between the antenna elements. The variation in the radiated power ratio can also be made very uniform over a large range of thickness of the DNG shell, easing the practical design of the shell. This is achieved by filling the region surrounding the dipole array with a material of non-unity permittivity and optimizing the media parameters. This uniformity in the radiated power ratio characteristics with variation in the metamaterial shell thickness eliminates the major drawback referred to previously where extremely thin metamaterial shells needed to be synthesized for high radiated power ratio. The frequency response of the system is investigated using the Drude model.

#### References

1. R.W. Ziolkowski, A.D. Kipple, IEEE Trans. Antennas Propag. **51**, 2626–2640 (2003)
2. R.W. Ziolkowski, A. Erentok, IEEE Trans. Antennas Propag. **54**, 2113–2130 (2006)

3. A. Erentok, R.W. Ziolkowski, *IEEE Trans. Antennas Propag.* **55**, 731–741 (2007)
4. R.W. Ziolkowski, A. Erentok, *IET Microw. Antennas Propag.* **1**, 116–128 (2007)
5. B. Ghosh, S. Ghosh, A.B. Kakade, *Phys. Rev. E* **78**, 026611-1–026611-13 (2008)
6. R.A. Shelby, D.R. Smith, S.C. Nemat-Nasser, S. Schultz, *Appl. Phys. Lett.* **78**, 489–491 (2001)
7. R.W. Ziolkowski, *IEEE Trans. Antennas Propag.* **51**, 1516–1529 (2003)
8. R.F. Harrington, *Time Harmonic Electromagnetic Fields* (McGraw-Hill, New York, 1961)
9. S. Arslanagic, R.W. Ziolkowski, O. Breinbjerg, *Radio Sci.* **42**, 1–20 (2007)

Copyright of Applied Physics A: Materials Science & Processing is the property of Springer Science & Business Media B.V. and its content may not be copied or emailed to multiple sites or posted to a listserv without the copyright holder's express written permission. However, users may print, download, or email articles for individual use.